Near Spectroscopically Accurate Ab Initio Potential Energy Surface for NH 4 + and Variational Calculations of Low-Lying Vibrational Levels

ARTICLE *in* THE JOURNAL OF PHYSICAL CHEMISTRY A · MARCH 2015

Impact Factor: 2.69 · DOI: 10.1021/acs.jpca.5b01835 · Source: PubMed

4 AUTHORS, INCLUDING:

Hongwei Song

Nanyang Technological University

12 PUBLICATIONS **52** CITATIONS

SEE PROFILE

Jun Li

Chongqing University

61 PUBLICATIONS **756** CITATIONS

SEE PROFILE

Hua Guo

University of New Mexico

382 PUBLICATIONS **7,533** CITATIONS

SEE PROFILE

THE JOURNAL OF PHYSICAL CHEMISTRY A

Article

pubs.acs.org/JPCA

Near Spectroscopically Accurate Ab Initio Potential Energy Surface for NH_4^+ and Variational Calculations of Low-Lying Vibrational Levels

Huixian Han,[†,‡] Hongwei Song,[†] Jun Li,[§] and Hua Guo*[,†]

[†]Department of Chemistry and Chemical Biology, University of New Mexico, Albuquerque, New Mexico 87131, United States

[‡]School of Physics, Northwest University, Xi'an, Shaanxi 710069, China

[§]School of Chemistry and Chemical Engineering, Chongqing University, Chongqing 400030, China

ABSTRACT: A nine-dimensional potential energy surface (PES) for the ammonium cation has been constructed by fitting ~30 000 AE-CCSD(T)-F12a/cc-pCVTZ-F12 points up to 32 262 cm^{-1} (4.0 eV) from the minimum. The fitting using the permutation invariant polynomial-neural network method has high fidelity, with a root-mean-square error of merely 2.34 cm^{-1}. The low-lying vibrational energy levels of NH_4^+ have been determined quantum mechanically using both Jacobi and normal coordinates, and the fundamental frequencies are in excellent agreement with available experimental data.

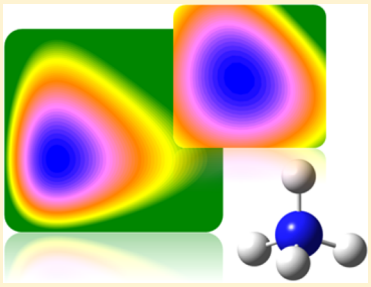

I. INTRODUCTION

On the basis of the separation of electronic and nuclear motions, the Born−Oppenheimer approximation attributes the ro-vibrational spectrum of a molecule to nuclear dynamics on its potential energy surface (PES). As a result, the Born−Oppenheimer PES is of central importance in molecule spectroscopy.[1,2] Earlier efforts to determine PESs were mostly devoted to the empirical construction of force fields, which are essentially a Taylor expansion of the PES near the equilibrium geometry, from experimental vibrational band origins.[3] With the advent of high-level electronic structure methods, ab initio force fields have become increasingly popular and their accuracy for small molecules has reached an unprecedented level.[4,5] However, this force-field approach is inherently limited to the configuration space near the equilibrium geometry and may fail in regions where high-order anharmonicity is strong.

Perhaps the ultimate and general approach to molecular spectroscopy is to develop global PESs using high-level ab initio methods followed by an exact calculation of the ro-vibrational levels using quantum mechanics. Ideally, such a first-principles approach introduces no bias and has thus the hope to predict all energy levels with equal accuracy. Indeed, significant advances have been made with the recursive methods for solving the nuclear Schrödinger equation so that highly excited energy levels of polyatomic molecules such as CH_4 can now be routinely computed on a given PES.[6−8] However, it is still quite challenging to represent accurately the multidimensional PES in an analytical form from ab initio points, even when electronic structure methods have advanced to a level close to spectroscopic accuracy (~1 cm^{-1}).[9−12] Besides the high fidelity in representing the ab initio points, a key point in constructing Born−Oppenheimer PESs is the treatment of the permutation symmetry. The invariance of the PES with respect to any permutation of identical atoms in the molecule needs be strictly observed if the correct spectroscopic information is to be expected.[13] This problem is particularly acute for hydrates such as CH_4 and NH_4^+, which have 4! = 24 possible permutations. Although such permutation invariance can be readily imposed in force fields, the adaptation of symmetry in a general PES is not as straightforward as it seems. Bowman and co-workers have recently proposed a permutation invariant polynomial (PIP) approach,[14,15] which enforces permutation symmetry using PIPs. This method is simple and rigorous, resulting in accurate PESs for systems with a large number of identical atoms, such as H_3O^+, H_5^+, and H_7^+.[16−18] We have also proposed a neural network (NN) method with low-order PIPs as the input layer to enforce the permutation symmetry.[19,20] This so-called PIP-NN method has been successfully applied to several systems with unprecedented high fitting fidelity while preserving permutation invariance.[12,21−26] For example, we have recently reported a global PES for the isomerization between acetylene (HCCH) and vinylidine (H_2CC) with a root-mean-square error (RMSE) of <10 cm^{-1}, which was shown to predict the experimentally observed normal-to-local transition in the bending modes up to 15 000 cm^{-1} above the zero-point energy level.[26] In another study, a nine-dimensional global reactive PES with an RMSE of 27 cm^{-1} was devised for the neutral ammonium radical (NH_4), including its dissociation asymptotes.[22] The combination of highly accurate ab initio calculations and high-fidelity representation of the PES has the promise to provide a true first-principles understanding of molecular vibration with spectroscopic accuracy. In this work, we report a new semiglobal PES for the ammonium cation (NH_4^+) based on explicitly correlated coupled cluster singles

Received: February 24, 2015
Revised: March 16, 2015
Published: March 17, 2015

DOI: 10.1021/acs.jpca.5b01835
J. Phys. Chem. A 2015, 119, 3400−3406

Table 1. Comparison of Ab Initio and PES Values for the Equilibrium N−H Distance (Angstrom), Ionization Potential (eV), and Harmonic Frequencies (cm^{-1}) with Available Experimental and Theoretical Data

	r_e	IP	ω_1	ω_2	ω_3	ω_4
FC-F12a/AVTZ	1.0216	4.672	3385.0	1740.2	3507.1	1489.6
FC-F12a/AVQZ	1.0212	4.672	3388.5	1741.4	3511.1	1490.5
FC-F12a/cc-pCVTZ-F12	1.0214	4.622	3386.2	1741.5	3508.8	1490.8
FC-F12a/cc-pCVQZ-F12	1.0212	4.598	3388.0	1741.8	3510.6	1490.7
AE-F12a/cc-pCVTZ-F12	1.0205	4.615	3391.2	1742.5	3513.5	1492.3
AE-F12a/cc-pCVQZ-F12	1.0202	4.591	3393.2	1743.0	3515.5	1492.6
theory[a]			3388.0	1743.0	3509.0	1491.0
theory[b]	1.0203					
theory[c]	1.0217					
theory (best estimate)[d]	1.0203		3394.7	1742.9	3516.1	1492.8
PIP-NN PES	1.0204		3392.4	1742.8	3513.9	1492.5
experiment	1.0208 ± 0.0020[e]	5.9 ± 0.5[f]				
		4.6 ± 0.2[g]				
		4.73 ± 0.06[h]				

[a]Ref 38. [b]Ref 37. [c]Ref 36. [d]Ref 4. [e]Ref 33 (an estimate from the experimental r_0). [f]Ref 46. [g]Ref 47. [h]Ref 48.

and doubles with perturbative triples (CCSD(T)-F12a) calculations.

The ammonium cation is an important species in chemistry and biology. It is stable not only in solutions but also in the gas phase. In plasmas containing hydrogen and nitrogen, for example, NH_4^+ has been found to be the dominant ion.[27] This molecular ion has also been found in space recently.[28] While the vibrational population in the latter case is most likely restricted to the lowest levels, the level of excitation in the vibrational degrees of freedom in a plasma is expected to be quite high. Some of its vibrational bands have been observed in spectroscopic experiments.[29−35] In particular, the ν_3 mode of NH_4^+ was first detected by Crofton and Oka[29] and by Saykally and co-workers.[30] The ν_4 band was later identified by Polak et al.[34] and by Park et al.[35] Spectral lines of several isotopomers have also been reported.[32,33] Theoretically, several authors have computed its equilibrium geometry or harmonic frequencies.[36−38] Martin and Lee reported an accurate ab initio quartic force field for this ion and calculated vibrational frequencies for NH_4^+ and deuterated isotopomers.[4] Best estimates were given for the equilibrium geometry and fundamental frequencies, and the agreement with available experimental data was quite good. In this work, we report a semiglobal PES for NH_4^+ with a PIP-NN fit of ∼30 000 high-level ab initio points up to 32 262 cm^{-1} above the potential minimum and variational calculations of the low-lying vibrational levels on the PES. Such a PES is not only important for fundamental studies of this molecular ion but also might be useful in assigning highly excited vibrational levels of NH_4^+ in plasma environments.

II. THEORY

II.A. Ab Initio Calculations. All ab initio calculations were performed with the MOLPRO package,[39] using the explicitly correlated (F12) CCSD(T) method.[40,41] The CCSD(T) method is used because of its ability to capture accurately the electron correlation energy, which is important for achieving spectroscopic accuracy. There is ample evidence indicating that F12 methods offer much faster convergence with respect to the size of the basis set.[40,41] To determine the basis set needed for generating the ab initio points, the equilibrium geometry and harmonic frequencies of NH_4^+ were first calculated at the CCSD(T)-F12a level with several basis sets, including the aug-cc-pVXZ (X=T,Q) basis sets of Dunning and co-workers (AVXZ)[42,43] and cc-pCVXZ-F12(X=T,Q) basis sets of Peterson and co-workers.[44,45] In these calculations, both frozen-core (FC) and all-electron (AE) treatments were employed.

NH_4^+ is isoenergetic with CH_4 with 10 electrons. Indeed, all optimization yielded a T_d equilibrium geometry for NH_4^+, although no symmetry restriction was imposed. This high-symmetry equilibrium geometry is consistent with both experimental and previous theoretical results. The calculated equilibrium N−H distance, ionization potential (IP), and harmonic frequencies of NH_4^+ are compared in Table 1 with previous theoretical results[4,36−38] and available experimental data.[33,46−48] It is clear from the comparison that the calculated N−H equilibrium distance is in good agreement with experiment and best theoretical estimates at all levels. In addition, our values for the IP calculated by various basis sets are consistent with the experimental values,[46−48] although the latter are quite scattered. From Table 1, it is clearly seen that the core electron correlation has a noticeable effect on harmonic frequencies of this system. The results at the AE-CCSD(T)-F12a level represent an improvement over those at the FC-CCSD(T)-F12a level and are closer to the best estimates of Martin and Lee using the CCSD(T) method with extrapolation to the complete basis set limit and core correlation.[4] Consequently, the AE-CCSD(T)-F12a/cc-pCVTZ-F12 level was chosen to compute the energies of all ab initio points.

II.B. Potential Energy Surface Fitting. In sampling the ab initio points, the following procedure was followed. First, points were sampled in internal coordinates in the following range: $R_{NH} \in [0.8, 2.5]$ Å, $\theta_{HNH} \in [60°, 180°]$, and $\varphi_{HNHH} \in [40°, 170°]$. This region covers the equilibrium geometry and its surrounding area. These points allow the establishment of a primitive PES. On this PES, batches of trajectories at various energies were dispatched in searching of unphysical regions of the PES that resulted from the lack of ab initio data points. New points that were sufficiently far from the existing points (χ > 0.05 Å) were retained in the updated data set, and the closeness between a new point $\{\vec{d}_i\}$ and one in the data set $\{\vec{d}_i'\}$ was judged by $\chi(\vec{d}_i) = (\sum_{i=1}^{10} |\vec{d}_i - \vec{d}_i'|)^{1/2}$. All permutation equivalent points were included in such screenings. This process was iterated until no new points could be

DOI: 10.1021/acs.jpca.5b01835
J. Phys. Chem. A 2015, 119, 3400−3406

added. A total of 29 214 points below 32 262 cm^{-1} relative to the potential minimum were selected, as the CCSD(T) approach is not expected to be accurate for describing fragmentation of the molecule to $NH_3 + H^+$, which is about 71 783 cm^{-1}.[49] An accurate global PES including the dissociation limits would require a multireference treatment.[12]

Neural networks have been used to provide an efficient and accurate representation of PESs.[50−53] Our permutation invariant polynomial−neural network (PIP-NN) approach[19,20] has been used with great success in fitting PESs with average errors on the order of a few meV or less. In the PIP-NN approach, low-order PIPs were used as symmetry functions in the input layer of the NN in order to enforce the permutation invariance of the PES. They replace the nine internal coordinates normally used in NN fits. The PIP functions of the following form were used:[54]

$$G = \hat{S} \prod_{i<j}^{N} p_{ij}^{l_{ij}} \tag{1}$$

where N is the number of atoms. $p_{ij} = \exp(-\alpha r_{ij})$ are the Morse-like variables with α as an adjustable constant and r_{ij} being the $N(N-1)/2$ internuclear distances.[14] l_{ij} is the degree of p_{ij}, and $M = \sum_{i<j}^{N} l_{ij}$ is the total degree in each monomial. $\hat{S}$ is the symmetrization operator, which consists of all 24 permutation operations in NH_4^+. To ensure the true permutation symmetry, all 208 PIPs up to the fifth order have been included. The redundancy causes no numerical problems.

In the NN fitting, two hidden layers were considered, which are denoted by (N1−N2) with N1 and N2 as the numbers of neurons in each layer. All NN fittings were performed using the Levenberg−Marquardt algorithm,[55] with the following RMSE as the penalty function:

$$\mathrm{RMSE} = \sqrt{\frac{1}{n}\sum_{i=1}^{n} (E_{\mathrm{fit}} - E_{\mathrm{calc}})^2} \tag{2}$$

In the NN fitting, the data were divided randomly into three sets, namely, the training (90% of the data points), validation (5%), and test (5%) sets. Only fits with similar RMSEs for all three sets were accepted in order to avoid false extrapolation due to edge points in the randomly selected validation and test sets. In addition, the maximum deviation is also used in selecting the final PIP-NN fits. For each NN architecture, 50 different training calculations were performed and the "early stopping" method[50] was employed to avoid overfitting. The final PIP-NN PES was chosen by the NN ensemble approach as the average of three best fits in order to further reduce random errors.

II.C. Exact Calculation of Vibrational Levels. The nine-dimensional Hamiltonian for the penta-atomic system ABCDE in the Jacobi coordinates, as shown in Figure 1, for vanishing total angular momentum $J_{\mathrm{tot}} = 0$ takes the following form ($\hbar = 1$ hereafter):[56,57]

$$\hat{H} = \sum_{i=0}^{3} \hat{h}_i(r_i) + \frac{\hat{j}^2}{2\mu_0 r_0^2} + \frac{\hat{l}_1^2}{2\mu_1 r_1^2} + \frac{\hat{l}_2^2}{2\mu_2 r_2^2} + \frac{\hat{j}_3^2}{2\mu_3 r_3^2} + \hat{V}(\vec{r_0}, \vec{r_1}, \vec{r_2}, \vec{r_3}) - \sum_{i=0}^{3} V_i^{\mathrm{ref}}(r_i) \tag{3}$$

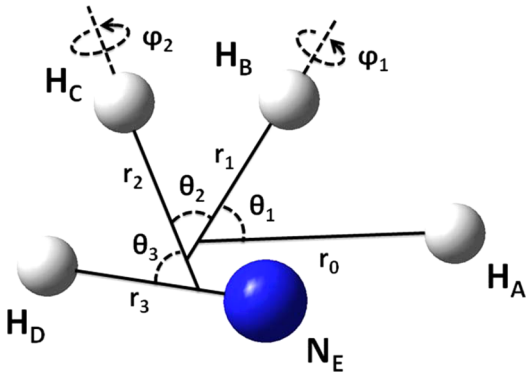

Figure 1. Nine-dimensional Jacobi coordinates for the ABCDE system.

where μ_0 is the reduced mass between A and BCDE, μ_1 is the reduced mass between B and CDE, μ_2 is the reduced mass between C and DE, and μ_3 is the reduced mass of DE. $\hat{j}_3$ is the rotational angular momentum operator of DE, and $\hat{l}_2$ is the orbital angular momentum operator of atom C with respect to DE. $\hat{j}_{23}$ is the angular momentum operator of CDE, which is coupled by $\hat{j}_3$ and $\hat{l}_2$. $\hat{l}_1$ is the orbital angular momentum operator of atom B with respect to CDE. $\hat{J}$ is coupled by $\hat{l}_1$ and $\hat{j}_{23}$. $\hat{h}_i(r_i)$ is the one-dimensional (1D) reference Hamiltonian, which is defined as

$$\hat{h}_i(r_i) = -\frac{1}{2\mu_i}\frac{\partial^2}{\partial r_i^2} + V_i^{\mathrm{ref}}(r_i), \quad i = 0, 3 \tag{4}$$

where $V_i^{\mathrm{ref}}(r_i)$ is the corresponding 1D reference potential.

The discretization of the wave function follows our earlier work[58] and thus is not discussed here. Briefly, the radial basis is a direct product of potential-optimized discrete variable representation (PODVR) functions,[59,60] while the angular basis is constructed by parity-adapted angular momentum eigenfunctions in the body-fixed (BF) framework. The angular wave function is transformed between the finite basis representation (FBR) and discrete variable representation (DVR) via a series of one-dimensional pseudospectral transformations.[61] The Lanczos algorithm in the parallel ARPACK software package[62] was utilized to calculate the bound states by providing our own subroutines to perform matrix vector multiplication. The action of the Hamiltonian on the FBR wave function is evaluated with a partial sum.[63] To compute the action of the potential energy operator, the FBR wave function is converted to DVR, in which the potential matrix, **V**, is diagonal.[64]

The method outlined above is exact in form, but the size of the basis is quite large for spectroscopic convergence with our current computational power. As discussed later, the degeneracy of the vibrational modes is not strictly achieved. We note in passing that schemes exist for reducing the size of the problem,[65−68] which should afford better convergence.

II.D. MULTIMODE Calculations of Vibrational Levels. The MULTIMODE approach,[69] which is based on the Watson Hamiltonian,[70] was also employed to compute the vibrational energy levels ($J_{\mathrm{tot}} = 0$) of NH_4^+ on the earlier-described PES. Because it has been discussed extensively in the literature,[69] few details are given here. Briefly, the mass-scaled normal mode coordinates were used in the Hamiltonian. The vibrational wave function is expressed as an expansion of direct-product basis functions, while the potential is expanded as a hierarchical

DOI: 10.1021/acs.jpca.5b01835
J. Phys. Chem. A 2015, 119, 3400−3406

n-mode representation. The calculations were performed with a truncated potential with up to six-mode terms. The vibrational problem was first solved using the vibrational self-consistent field (VSCF) approach,[71,72] and then the vibrational wave functions were further expanded in terms of the eigenfunctions of the VSCF Hamiltonian to account for coupling among the nine vibrational modes. This virtual configuration interaction (VCI) method[73,74] improves the results significantly. The maximum number of coupled modes allowed in the basis in MULTIMODE is 5. The maximum sum of quanta was taken to be 8 for one-, two-, three-, four-, and five-mode excitations, and the maximum allowed quanta in mode i for one- to five-mode excitations was set to 8, 7, 6, 5, and 4, respectively. For present calculations, the molecules are treated within C_1 symmetry. Convergence tests suggest that the fundamental vibrational frequencies (ν_1, ν_2, ν_3, and ν_4) are converged to ~0.1 cm^{-1}.

III. RESULTS AND DISCUSSION

In the PIP-NN fitting, several two-layer NN structures with different numbers of neurons were tested. The final structure consists of a two-layer NN with 20 and 50 neurons, NN (20−50) with 5 261 parameters. The RMSEs for the training, validation, and testing sets and the maximum deviation of the three best PESs are 2.34/6.05/5.24/99.29, 2.58/4.44/5.57/44.52, and 3.15/5.40/7.10/49.60 cm^{-1}, respectively. The final PES has a total RMSE of 2.33 cm^{-1} and a maximum deviation of 55.01 cm^{-1}. The distribution of the fitting errors for the final PES is shown in Figure 2. The PES can be obtained upon request from the corresponding author.

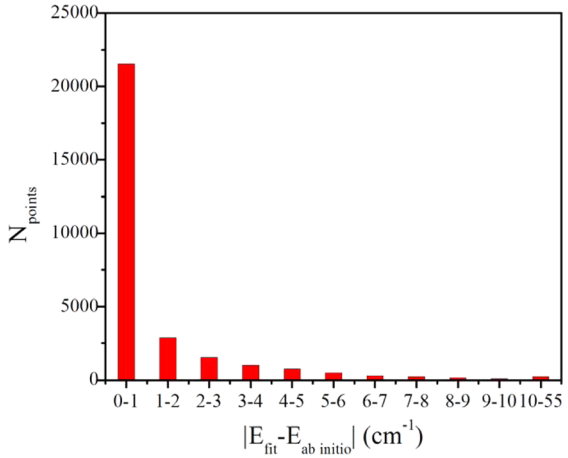

Figure 2. Distribution of the fitting errors for the selected points in the PIP-NN (20−50) PES.

In Figure 3, the contours of the PES are plotted. In panel (a), the x axis is one R_{NH} bond length (N−H1) and the y axis is another R_{NH} bond length (N−H2), with the latter forced to be equal to the two remaining R_{NH} bond lengths (N−H3 and N−H4). The remaining internal coordinates are optimized. In panel (b), the x axis is one θ_{HNH} angle (H1−N−H2) and the y axis is another θ_{HNH} angle (H1−N−H3), while all other internal coordinates are optimized. The minimum is clearly visible in the figures.

As shown in Table 1, the equilibrium geometry of the PES (R_{NH} = 1.0204 Å) is in good agreement with the ab initio value (R_{NH} = 1.0205 Å), which also agrees well with the experiment (R_{NH} = 1.0208(20) Å). The T_d molecule is isoelectronic with

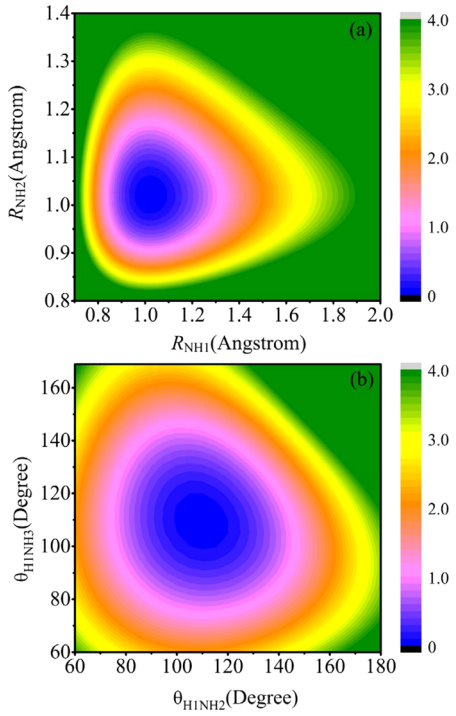

Figure 3. Contours of the PIP-NN PES: (a) as a function of R_{NH1} and R_{NH2}, retaining $R_{NH2} = R_{NH3} = R_{NH4}$ with all other internal coordinates optimized, and (b) along θ_{H1NH2} and θ_{H1NH3}, with all other internal coordinates optimized.

CH_4 and has four vibrational modes. A vibrational level is customarily denoted as $(n_1n_2n_3n_4)$, where the quantum numbers are for the symmetric stretching, bending, antisymmetric stretching, and umbrella modes, respectively. These normal modes have 1, 2, 3, and 3-fold degenerate, often labeled by the symmetry species to which they belong (A_1, E, F_2, and F_2). The harmonic vibrational frequencies of PES have been computed by using POLYRATE 9.7.[75] The energies among the degenerate modes differ at most in the second decimal. As listed in Table 1, they are also in good agreement with those directly computed ab initio. The maximum deviation between our results and the best theoretical estimate[4] is only 2.3 cm^{-1}.

Low-lying vibrational levels of NH_4^+ have been computed using the two quantum mechanical methods described earlier. The numerical parameters used in the Lanczos calculations are listed in Table 2. In these calculations, the number of the

Table 2. Numerical Parameters Used in the Full-Dimensional Quantum Bound State Calculations under the Jacobi Coordinates

grid/basis range and size	$N_{r_0} = N_{r_1} = N_{r_2} = N_{r_3} = 5$
	$l_{1max} = l_{2max} = l_{3max} = 22$
	$j_{23max} = 34$, $J_{max} = 28$

angular basis functions is 1 473 687 and the number of grid points in integrating the angular coordinates is 12 592 845, resulting in a total of about 9.21 × 10^8 basis functions and 7.87 × 10^9 grid points. The calculation was carried out on a distributed-memory cluster with 136 cores (Intel Xeon CPU E5540 @ 2.53 GHz). The total CPU time consumed is around 1762.82 h. The resulting size of VCI matrix for J_{tot} = 0 is 21 661

DOI: 10.1021/acs.jpca.5b01835
J. Phys. Chem. A 2015, 119, 3400−3406

for all isotopomers, and the total CPU time for each species is around 7−8 h (Intel Xeon CPU E5−2670 0 @ 2.60 GHz).

The results for fundamental levels are compared with available experimental data in Table 3. The energies of fundamentals calculated by the two approaches are almost identical to each other, and the ZPE values differ by 1.3 cm^{-1}. They are also in good agreement with available experimental data. The discrepancies between our MULTIMODE (Lanczos) results and experimental values are 0.56 (1.36) and 0.32 (0.22) cm^{-1} for ν_3 and ν_4 modes, respectively.

Table 3. Comparison of the Calculated Fundamental Frequencies (cm^{-1}) of NH_4^+ with Available Experimental and Theoretical Data

	experiment	theory (best estimate)[a]	normal[b] (PIP-NN PES)	Jacobi[c] (PIP-NN PES)
ZPE			10763.8	10765
ν_1		3236.6	3237.2	3238
ν_2		1690.1	1691.5	1692
ν_3	3343.14[d]	3345.1	3343.7	3345
ν_4	1447.22[e]	1447.2	1446.9	1447

[a]Ref 4. [b]Using the MULTIMODE approach. [c]Using the Lanczos approach. [d]Ref 31. [e]Ref 34.

In the Lanczos calculations using the Jacobi coordinates and the MULTIMODE calculations using normal coordinates, the energies of degenerate levels are within 1.0 and 0.1 cm^{-1}, respectively. The small errors among the degenerate levels can be attributed to the insufficient basis used in these calculations.

Table 4 lists the calculated zero-point energies as well as harmonic and fundamental frequencies of several isotopomers of NH_4^+. All harmonic frequencies are from the CCSD(T)/cc-pVTZ[4] and AE-CCSD(T)-F12a/cc-pCVTZ-F12 calculations. Fundamental frequencies are calculated using CCSD(T)/cc-pVTZ and the MULTIMODE approach based on PIP-NN PES. Except for ω_2 and ν_2 of $NH_2D_2^+$, and ω_4 of NHD_3^+ with relatively large deviations (62.1, 33.0, and 56.9 cm^{-1}, respectively), the other harmonic and fundamental frequencies are in accordance with previous theoretical data.[4] Indeed, it can be seen from Table 4 that our calculated fundamental frequencies of ν_4 = 3341.5 cm^{-1} for NH_3D^+ and ν_3 = 2495.1 cm^{-1} for ND_4^+ are closer to the only available experimental values,[32,33] with deviations of 0.42 and 1.06 cm^{-1}, respectively.

IV. CONCLUSIONS

In this work, we report a nine-dimensional semiglobal PES for the ammonium molecular cation. The NH_4^+ is an important species in solution chemistry and also plays an important role in gas-phase environments. In particular, it has been found to be the dominant ion in the plasma-assisted ammonia synthesis from H_2/N_2 mixtures.[27] As a result, the highly vibrationally excited states are of great importance for diagnostics of the plasma. The PES reported here is a high-fidelity PIP-NN fit of ∼30 000 points at the AE-CCSD(T)-F12a/cc-pCVTZ-F12 level with a fitting error on the order of 2 cm^{-1}. In addition to the excellent agreement with the experimental geometry of this T_d molecular ion, the harmonic vibrational frequencies are also in good accord with the best theoretical estimate.[4] The accuracy of the PES is supported by two independent quantum mechanical calculations of the fundamental frequencies and the ZPE for NH_4^+, which are in excellent agreement with available experimental data. This level of agreement is particularly satisfactory as no empirical adjustment was included. The ZPE and the fundamental frequencies of several isotopomenrs of NH_4^+ are also calculated and discussed. This and other recent

Table 4. Zero-Point Energies (ZPEs in cm^{-1}) and Harmonic (ω) and Fundamental (ν) Frequencies (in cm^{-1}) of Isotopologues NH_3D^+, $NH_2D_2^+$, NHD_3^+, ND_4^+, and $^{15}ND_4^+$

	NH_3D^+		$NH_2D_2^+$		NHD_3^+		ND_4^+		$^{15}ND_4^+$
	this work[a]	Martin and Lee[b]	this work[a]	Martin and Lee[b]	this work[a]	Martin and Lee[b]	this work[a]	Martin and Lee[b]	this work[a]
ZPE[c]	10227.6		9494.8		8752.3		7997.5		7965.2
ω_1	3426.5	3423.7	3458.0	3454.9	3486.8	3483.4	2399.1	2397.3	2399.1
ω_2	2537.8	2535.1	2489.3	2427.2	2443.4	2441.2	1232.7	1233.4	1232.8
ω_3	1486.6	1486.1	1632.8	1633.4	1128.8	1128.3	2589.4	2586.4	2575.6
ω_4	3513.5	3510.0	1163.1	1163.1	2589.5	2532.6	1120.7	1120.4	1113.0
ω_5	1674.1	1674.7	1509.2	1510.2	1466.5	1466.6			
ω_6	1314.4	1314.0	3513.4	3509.9	1166.8	1166.6			
ω_7			1231.7	1231.3					
ω_8			2589.4	2586.4					
ω_9			1402.8	1402.4					
ZPE[d]	10064.5		9353.2		8630.8		7897.8		7866.3
ν_1	3284.2	3297.7	3297.9	3297.9	3317.1	3311.4	2328.7	2325.9	2327.2
ν_2	2435.5	2430.8	2426.5	2393.5	2371.3	2370.5	1206.1	1205.8	1206.2
ν_3	1443.0	1442.4	1584.2	1583.7	1101.4	1101.0	2495.1[f]	2492.0	2482.4
ν_4	3341.5[e]	3336.6	1136.3	1136.1	2484.4	2479.2	1095.2	1094.9	1087.8
ν_5	1624.5	1624.2	1469.6	1469.2	1426.9	1426.9			
ν_6	1278.6	1278.6	3338.1	3333.4	1140.3	1140.6			
ν_7			1198.8	1198.7					
ν_8			2465.8	2461.8					
ν_9			1364.0	1363.5					

[a]Harmonic frequencies at the AE-CCSD(T)-F12a/cc-pCVTZ-F12 level; fundamental frequencies obtained using the MULTIMODE approach on PIP-NN PES. [b]Ref 4 at the CCSD(T)/cc-pVTZ level. [c]ZPE at the AE-CCSD(T)-F12a/cc-pCVTZ-F12 level. [d]ZPE obtained with the MULTIMODE approach on PIP-NN PES. [e]Experimental value is 3341.076 cm^{-1}.[32] [f]Experimental value is 2494.0421(50) cm^{-1}.[33]

DOI: 10.1021/acs.jpca.5b01835
J. Phys. Chem. A 2015, 119, 3400−3406

work suggest that a first-principles determination of molecular spectra is quickly becoming a reality.

AUTHOR INFORMATION

Corresponding Author

*E-mail: hguo@unm.edu.

Notes

The authors declare no competing financial interest.

ACKNOWLEDGMENTS

This work is supported by the U.S. Department of Energy (DE-FG02-05ER15694 to H.G.). H.H. thanks research funding from the National Natural Science Foundation of China (Grant No. 21103136) and a scholarship from the Chinese Scholarship Council. J.L. was supported by the Hundred-Talent Foundation of Chongqing University (Project no. 0220001104420).

REFERENCES

(1) Murrell, J. N.; Carter, S.; Farantos, S. C.; Huxley, P.; Varandas, A. J. C. *Molecular Potential Energy Functions*; Wiley: Chichester, U.K., 1984.

(2) Schatz, G. C. The Analytical Representation of Electronic Potential-Energy Surfaces. *Rev. Mod. Phys.* **1989**, *61*, 669.

(3) Wilson, E. B.; Decius, J. C.; Cross, P. C. *Molecular Vibrations*; Dover: New York, 1955.

(4) Martin, J. M. L.; Lee, T. J. Accurate Ab Initio Quartic Force Field and Vibrational Frequencies of the NH_4^+ Ion and Its Deuterated Forms. *Chem. Phys. Lett.* **1996**, *258*, 129−135.

(5) Martin, J. M. L.; Lee, T. J. A Purely Ab Initio Spectroscopyic Quality Quartic Force Field for Acetylene. *J. Chem. Phys.* **1998**, *108*, 676.

(6) Carrington, T., Jr. Methods for Calculating Vibrational Energy Levels. *Can. J. Chem.* **2004**, *82*, 900.

(7) Guo, H. Recursive Solutions to Large Eigenproblems in Molecular Spectroscopy and Reaction Dynamics. *Rev. Comput. Chem.* **2007**, *25*, 285−347.

(8) Bowman, J. M.; Carrington, T.; Meyer, H.-D. Variational Quantum Approaches for Computing Vibrational Energies of Polyatomic Molecules. *Mol. Phys.* **2008**, *106*, 2145−2182.

(9) Yurchenko, S. N.; Tennyson, J. Exomol Line Lists. IV. The Rotation-Vibration Spectrum of Methane up to 1500 K. *Mon. Not. R. Astron. Soc.* **2014**, *440*, 1649−1661.

(10) Rey, M.; Nikitin, A. V.; Tyuterev, V. G. Theoretical Hot Methane Line Lists up to T = 2000 K for Astrophysical Applications. *Astrophys. J.* **2014**, *789*.

(11) Wang, X.-G.; Carrington, T. Using Experimental Data and a Contracted Basis Lanczos Method to Determine an Accurate Methane Potential Energy Surface from a Least Squares Optimization. *J. Chem. Phys.* **2014**, *141*, 154106.

(12) Majumder, M.; Hegger, S. E.; Dawes, R.; Manzhos, S.; Wang, X.-G.; Carrington, T.; Li, J.; Guo, H. Explicitly-Correlated MRCI-F12 Potential Energy Surfaces for Methane Fit with Several Permutation Invariant Schemes and Full-Dimensional Vibrational Calculations. *Mol. Phys.* **2015**, DOI: 10.1080/00268976.2015.1015642.

(13) Bunker, P. R.; Jensen, P. *Molecular Symmetry and Spectroscopy*; NRC Research Press: Ottawa, Canada, 1998.

(14) Braams, B. J.; Bowman, J. M. Permutationally Invariant Potential Energy Surfaces in High Dimensionality. *Int. Rev. Phys. Chem.* **2009**, *28*, 577−606.

(15) Bowman, J. M.; Czakó, G.; Fu, B. High-Dimensional Ab Initio Potential Energy Surfaces for Reaction Dynamics Calculations. *Phys. Chem. Chem. Phys.* **2011**, *13*, 8094−8111.

(16) Huang, X.; Carter, S.; Bowman, J. M. Ab Initio Potential Energy Surface and Vibrational Energies of H_3O^+ and Its Isotopomers. *J. Phys. Chem. B* **2002**, *106*, 8182−8188.

(17) Xie, Z.; Braams, B. J.; Bowman, J. M. Ab Initio Global Potential-Energy Surface for $H_5^+ \rightarrow H_3^+ + H_2$. *J. Chem. Phys.* **2005**, *122*, 224307.

(18) Barragán, P.; Prosmiti, R.; Wang, Y.; Bowman, J. M. Full-Dimensional (15-Dimensional) Ab Initio Analytical Potential Energy Surface for the H_7^+ Cluster. *J. Chem. Phys.* **2012**, *136*, 224302.

(19) Jiang, B.; Guo, H. Permutation Invariant Polynomial Neural Network Approach to Fitting Potential Energy Surfaces. *J. Chem. Phys.* **2013**, *139*, 054112.

(20) Li, J.; Jiang, B.; Guo, H. Permutation Invariant Polynomial Neural Network Approach to Fitting Potential Energy Surfaces. II. Four-Atomic Systems. *J. Chem. Phys.* **2013**, *139*, 204103.

(21) Li, J.; Chen, J.; Zhang, D. H.; Guo, H. Quantum and Quasi-Classical Dynamics of the OH + CO → H + CO_2 Reaction on a New Permutationally Invariant Neural Network Potential Energy Surface. *J. Chem. Phys.* **2014**, *140*, 044327.

(22) Li, J.; Guo, H. A Nine-Dimensional Global Potential Energy Surface for $NH_4(X^2A_1)$ and Kinetics Studies on the H + $NH_3 \leftrightarrow H_2$ + NH_2 Reaction. *Phys. Chem. Chem. Phys.* **2014**, *16*, 6753−6763.

(23) Li, J.; Carter, S.; Bowman, J. M.; Dawes, R.; Xie, D.; Guo, H. High-Level, First-Principles, Full-Dimensional Quantum Calculation of the Ro-Vibrational Spectrum of the Simplest Criegee Intermediate (CH_2OO). *J. Phys. Chem. Lett.* **2014**, *5*, 2364−2369.

(24) Li, A.; Guo, H. A Nine-Dimensional Ab Initio Global Potential Energy Surface for the $H_2O^+ + H_2 \rightarrow H_3O^+ + H$ Reaction. *J. Chem. Phys.* **2014**, *140*, 224313.

(25) Li, A.; Guo, H. A Full-Dimensional Ab Initio Global Potential Energy Surface of $H_3O^+(\tilde{a}^3A)$ for the $OH^+(\tilde{X}^3\Sigma^-) + H_2(\tilde{X}^1\Sigma_g^+) \rightarrow H(^2S) + H_2O^+(\tilde{X}^2B_1)$ Reaction. *J. Phys. Chem. A* **2014**, *118*, 11168−11176.

(26) Han, H.; Li, A.; Guo, H. Towards Spectroscopically Accurate Global Ab Initio Potential Energy Surface for the Acetylene-Vinylidene Isomerization. *J. Chem. Phys.* **2014**, *141*, 244312.

(27) Carrasco, E.; Jimenez-Redondo, M.; Tanarro, I.; Herrero, V. J. Neutral and Ion Chemistry in Low Pressure DC Plasmas of H_2/N_2 Mixtures: Routes for the Efficient Production of NH_3 and NH_4^+. *Phys. Chem. Chem. Phys.* **2011**, *13*, 19561−19572.

(28) Cernicharo, J.; Tercero, B.; Fuente, A.; Domenech, J. L.; Cueto, M.; Carrasco, E.; Herrero, V. J.; Tanarro, I.; Marcelino, N.; Roueff, E.; et al. Detection of the Ammonium Ion in Space. *Astrophys. J. Lett.* **2013**, *771*, L10.

(29) Crofton, M. W.; Oka, T. Infrared Studies of Molecular Ions. I. The ν_3 Band of NH_4^+. *J. Chem. Phys.* **1983**, *79*, 3157−3158.

(30) Schäfer, E.; Begemann, M. H.; Gudeman, C. S.; Saykally, R. J. The ν_3 Vibrational Spectrum of the Free Ammonium Ion (NH_4^+). *J. Chem. Phys.* **1983**, *79*, 3159−3160.

(31) Schäfer, E.; Saykally, R. J.; Robiette, A. G. A High Resolution Study of the ν_3 Band of the Ammonium Ion (NH_4^+) by Velocity Modulation Laser Absorption Spectroscopy. *J. Chem. Phys.* **1984**, *80*, 3969−3977.

(32) Nakanaga, T.; Amano, T. Difference-Frequency Laser Spectroscopy of the ν_3 Fundamental Band of NH_3D^+. *Can. J. Phys.* **1986**, *64*, 1356−1358.

(33) Crofton, M. W.; Oka, T. Observation of Forbidden Transitions of Ammonium Ion (NH_4^+) ν_3 Band and Determination of Ground State Rotational Constants. Observation of ν_3 Band Allowed Transitions of ND_4^+. *J. Chem. Phys.* **1987**, *86*, 5983−5988.

(34) Polak, M.; Gruebele, M.; DeKock, B. W.; Saykally, R. J. Velocity Modulation Infrared Laser Spectroscopy of Molecular Ions. *Mol. Phys.* **1989**, *66*, 1193−1202.

(35) Park, J.; Xia, C. H.; Selby, S.; Foster, S. C. The ν_4 Band of Ammonium, NH_4^+. *J. Mol. Spectrosc.* **1996**, *179*, 150−158.

(36) Peterson, K. A.; Xantheas, S. S.; Dixon, D. A.; Dunning, T. H. Predicting the Proton Affinities of H_2O and NH_3. *J. Phys. Chem. A* **1998**, *102*, 2449−2454.

(37) Demaison, J.; Margulès, L.; Boggs, J. E. The Equilibrium N−H Bond Length. *Chem. Phys.* **2000**, *260*, 65−81.

(38) Douguet, N.; Kokoouline, V.; Orel, A. E. Breaking a Tetrahedral Molecular Ion with Electrons: Study of NH_4^+. *J. Phys. B* **2012**, *45*, 051001.

DOI: 10.1021/acs.jpca.5b01835
J. Phys. Chem. A 2015, 119, 3400−3406

(39) Werner, H.-J.; Knowles, P. J.; Knizia, G.; Manby, F. R.; Schütz, M., et al. *MOLPRO2012 Molpro, version 2012.1, A Package of Ab Initio Programs*; http://www.molpro.net.
(40) Adler, T. B.; Knizia, G.; Werner, H.-J. A Simple and Efficient CCSD(T)-F12 Approximation. *J. Chem. Phys.* **2007**, *127*, 221106.
(41) Knizia, G.; Adler, T. B.; Werner, H.-J. Simplified CCSD(T)-F12 Methods: Theory and Benchmarks. *J. Chem. Phys.* **2009**, *130*, 054104.
(42) Dunning, T. H. Gaussian Basis Sets for Use in Correlated Molecular Calculations. I. The Atoms Boron through Neon and Hydrogen. *J. Chem. Phys.* **1989**, *90*, 1007−1023.
(43) Kendall, R. A.; Dunning, T. H.; Harrison, R. J. Electron Affinities of the First-Row Atoms Revisited. Systematic Basis Sets and Wave Functions. *J. Chem. Phys.* **1992**, *96*, 6796−6806.
(44) Peterson, K. A.; Adler, T. B.; Werner, H.-J. Systematically Convergent Basis Sets for Explicitly Correlated Wavefunctions: The Atoms H, He, B−Ne, and Al−Ar. *J. Chem. Phys.* **2008**, *128*, 084102.
(45) Hill, J. G.; Mazumder, S.; Peterson, K. A. Correlation Consistent Basis Sets for Molecular Core-Valence Effects with Explicitly Correlated Wave Functions: The Atoms B−Ne and Al−Ar. *J. Chem. Phys.* **2010**, *132*, 054108.
(46) Melton, C. E.; Joy, H. W. Mass Spectrometric and Theoretical Evidence for NH_4^+ and H_3O. *J. Chem. Phys.* **1967**, *46*, 4275−4283.
(47) Williams, B. W.; Porter, R. F. Energetics of Fragmentation of CH_5, H_3O, and NH_4 from Neutralized Ion-Beam Experiments. *J. Chem. Phys.* **1980**, *73*, 5598−5604.
(48) Gellene, G. I.; Cleary, D. A.; Porter, R. F. Stability of the Ammonium and Methylammonium Radicals from Neutralized Ion-Beam Spectroscopy. *J. Chem. Phys.* **1982**, *77*, 3471−3477.
(49) Kassab, E.; Evleth, E. M. Theoretical Study of the Ammoniated NH_4 Radical and Related Structures. *J. Am. Chem. Soc.* **1987**, *109*, 1653−1661.
(50) Raff, L. M.; Komanduri, R.; Hagan, M.; Bukkapatnam, S. T. S. *Neural Networks in Chemical Reaction Dynamics*; Oxford University Press: Oxford, U.K., 2012.
(51) Behler, J. Neural Network Potential-Energy Surfaces in Chemistry: A Tool for Large-Scale Simulations. *Phys. Chem. Chem. Phys.* **2011**, *13*, 17930−17955.
(52) Handley, C. M.; Popelier, P. L. A. Potential Energy Surfaces Fitted by Artificial Neural Networks. *J. Phys. Chem. A* **2010**, *114*, 3371−3383.
(53) Manzhos, S.; Dawes, R.; Carrington, T. Neural Network-Based Approaches for Building High Dimensional and Quantum Dynamics-Friendly Potential Energy Surfaces. *Int. J. Quantum Chem.* **2014**, DOI: 10.1002/qua.24795.
(54) Xie, Z.; Bowman, J. M. Permutationally Invariant Polynomial Basis for Molecular Energy Surface Fitting Via Monomial Symmetrization. *J. Chem. Theory Comput.* **2010**, *6*, 26−34.
(55) Hagan, M. T.; Menhaj, M. B. Training Feedforward Networks with the Marquardt Algorithm. *IEEE Trans. Neural Networks* **1994**, *5*, 989−993.
(56) Yang, M. Full Dimensional Time-Dependent Quantum Dynamics Study of the $H + NH_3 \rightarrow H_2 + NH_2$ Reaction. *J. Chem. Phys.* **2008**, *129*, 064315.
(57) Song, H.; Lee, S.-Y.; Yang, M.; Lu, Y. Full-Dimensional Quantum Calculations of the Vibrational States of H_5^+. *J. Chem. Phys.* **2013**, *138*, 124309.
(58) Song, H.; Li, J.; Yang, M.; Lu, Y.; Guo, H. Nine-Dimensional Quantum Dynamics Study of the $H_2 + NH_2 \rightarrow H + NH_3$ Reaction: A Rigorous Test of the Sudden Vector Projection Model. *Phys. Chem. Chem. Phys.* **2014**, *16*, 17770−17776.
(59) Wei, H.; Carrington, T., Jr. The Discrete Variable Representation of a Triatomic Hamiltonian in Bond Length Bond Angle Coordinates. *J. Chem. Phys.* **1992**, *97*, 3029.
(60) Echave, J.; Clary, D. C. Potential Optimized Discrete Variable Representation. *Chem. Phys. Lett.* **1992**, *190*, 225.
(61) Corey, G. C.; Tromp, J. W.; Lemoine, D. Fast Pseudospectral Algorithm Curvilinear Coordinates. In *Numerical Grid Methods and Their Applications to Schroedinger's Equation*; Cerjan, C., Ed.; Kluwer: Dordrecht, The Netherlands, 1993; pp 1−23.
(62) Lehoucq, R. B.; Sorensen, D. C.; Yang, C. *ARPACK User Guide: Solution of Large Scale Eigenvalue Problems by Implicitly Restarted Arnoldi Methods*; SIAM: Philadelphia, PA, 1998.
(63) Bramley, M. J.; Carrington, T., Jr. A General Discrete Variable Method to Calculate Vibrational Energy Levels of Three- and Four-Atom Molecules. *J. Chem. Phys.* **1993**, *99*, 8519−8541.
(64) Light, J. C.; Carrington, T., Jr. Discrete-Variable Representations and Their Utilization. *Adv. Chem. Phys.* **2000**, *114*, 263−310.
(65) Yu, H.-G. An Exact Variational Method to Calculate Vibrational Energies of Five Atom Molecules Beyond the Normal Mode Approach. *J. Chem. Phys.* **2002**, *117*, 2030.
(66) Yu, H.-G. A General Rigorous Quantum Dynamics Algorithm to Calculate Vibrational Energy Levels of Pentaatomic Molecules. *J. Mol. Spectrosc.* **2009**, *256*, 287−298.
(67) Wang, X.-G.; Carrington, T., Jr. A Contracted Basis-Lanczos Calculation of Vibrational Levels of Methane: Solving the Schrodinger Equation in Nine Dimensions. *J. Chem. Phys.* **2003**, *119*, 101.
(68) Wang, X.-G.; Carrington, T., Jr. A Finite Basis Representation Lanczos Calculation of the Bend Energy Levels of Methane. *J. Chem. Phys.* **2004**, *121*, 2937.
(69) Bowman, J. M.; Carter, S.; Huang, X. Multimode: A Code to Calculate Rovibrational Energies of Polyatomic Molecules. *Int. Rev. Phys. Chem.* **2003**, *22*, 533−549.
(70) Watson, J. K. G. Simplification of Molecular Vibration-Rotation Hamiltonian. *Mol. Phys.* **1968**, *15*, 479−490.
(71) Bowman, J. M. The Self-Consistent-Field Approach to Polyatomic Vibrations. *Acc. Chem. Res.* **1986**, *19*, 202−208.
(72) Ratner, M. A.; Gerber, R. B. Excited Vibrational States of Polyatomic Molecules: The Semiclassical Self-Consistent-Filed Approach. *J. Phys. Chem.* **1986**, *90*, 20−30.
(73) Carter, S.; Bowman, J. M. The Adiabatic Rotation Approximation for Rovibrational Energies of Many-Mode Systems: Description and Tests of the Method. *J. Chem. Phys.* **1998**, *108*, 4397−4404.
(74) Carter, S.; Bowman, J. M.; Handy, N. C. Extensions and Tests Of "Multimode": A Code to Obtain Accurate Vibration/Rotation Energies of Many-Mode Molecules. *Theor. Chem. Acc.* **1998**, *100*, 191−198.
(75) Corchado, J. C.; Chuang, Y.-Y.; Fast, P. L.; Hu, W.-P.; Liu, Y.-P.; Lynch, G. C.; Nguyen, K. A.; Jackels, C. F.; Fernandez Ramos, A.; Ellingson, B. A., et al. *Polyrate, version 9.7*; University of Minnesota: Minneapolis, MN, 2007.

DOI: 10.1021/acs.jpca.5b01835
J. Phys. Chem. A 2015, 119, 3400−3406